J KAU: Earth Sci., vol. 1, pp. 1-25 (1408A.H./1988A.D.)

Geochronology and Geochemical Evolution of the Wadi Turabah Felsic Plutonic Ring Complex, Central Arabian Shield

A.A. RADAIN, S. ALI and A.A. ABDEL-MONEM*
Faculty of Earth Sciences, King Abdulaziz University, P.O. Box 1744, Jeddah – 21441, Saudi Arabia.

ABSTRACT. Rb-Sr whole rock isochrons and major element oxide data for the Wadi Turabah felsic plutonic ring complex are discussed. Felsic rocks of the Wadi Turabah ring structure indicate a complex history of evolution and consist of gneissic granodiorite-granite suite (GGGS), massive granodiorite-granite suite (MGGS), and a ring dike granite. The GGGS and north trending metavolcanic and metasedimentary layered sequences (classified as Baish and Bahah) have suffered polyphase deformation and metamorphism in the upper and lower grades of the greenschist and amphibolite facies, respectively. The ring dike granite is the last phase in the magmatic evolution of the ring complex.

Rb-Sr whole rock data for six samples of the GGGS defines an apparent age of 535±11 Ma (2σ) with an initial $^{87}Sr/^{86}Sr$ ratio of 0.7037±0.00016 (2σ) and a MSWD (mean square of weighted deviates) value of 6.6. The age determined on five samples of MGGS is 416±9 Ma (2σ) with an initial $^{87}Sr/^{86}Sr$ ratio of 0.704±0.0002 (2σ) and a MSWD value of 9.01. The ring dike granite yields a four point isochron age of 117±0.4 Ma with an initial $^{87}Sr/^{86}Sr$ ratio of 0.7089±0.00015 (2σ) and a MSWD value of 0.01.

Major element oxide and Rb-Sr data indicate that the felsic plutonic rocks within the ring structure are highly differentiated and derived from fractional crystallization of magma generated from the lower crust or upper mantle. The chemical data also indicate that the ring dike granite is fractionated from magma of ternary minimum composition in the system SiO_2-$NaAlSiO_4$-$KAlSiO_4$ under water pressure of 1 Kb.

Introduction

Geological, geochemical, and geochronological studies carried out by different workers (Greenwood and Brown 1973, Greenwood *et al.* 1976, 1980, 1982, Fleck *et al.* 1980, Nasseef and Gass 1980, Roobol *et al.* 1983, Camp 1984, Stoeser and Camp 1984) on the western and southern parts of the Arabian Shield indicate that the protocontinental growth of the Shield in these parts, developed as a consequence of crustal plate tectonism. The result is reflected in the formation of ensimatic island arcs and active marginal arcs. At least, three ancient ensimatic island arcs are recognized in the western part of the shield with two suture zones (Fig. 1).

* Present address: Nuclear Material Corporation, Cairo, Egypt.

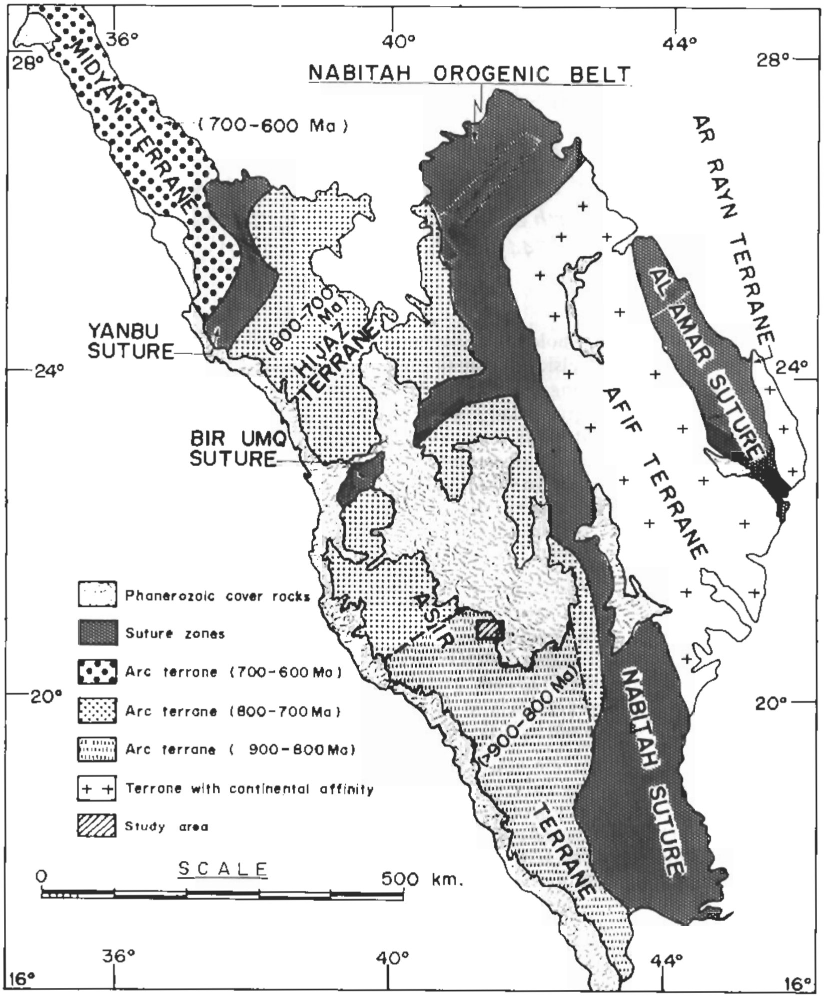

FIG. 1. Tectonic sketch map of the Arabian Shield (after Stoeser and Camp 1984).

Figure 2 is a simplified geological map of the southern part of the Asir microplate [arc terrane (>900-800)]. The oldest subduction related volcanism is indicated by the layered metavolcanic and metasedimentary sequences, occurring throughout the southern part of the Asir microplate. These layered rocks are assigned to the Baish and Bahah groups, and described in the literature by different names in different localities such as Metamorphic Unit 1 and Unit 2 in Wadi Shuqub quadrangle (Greene and Gonzalez 1980) and Bahah group in Jabal Ann quadrangle (Gonzalez 1973). In the Wadi Bidah region, this belt is well studied and referred to as; Metavolcanic and Metasedimentary rocks (Earhart and Mawad 1970), Sharq, Bidah, and Gharb groups (Jackaman 1972), Jof formation (Greenwood, 1975), Basaltic Assemblage (Fleck *et al.* 1980); Phase 1 (Hadley and Schmidt 1980), and Unit F and Unit E (Ramsay *et al.* 1981). This belt extends along Wadi Bidah in a north-trending direction. Some members of this belt are included within the studied circular intrusive structure to the north, and outside of which the belt trends north-north west.

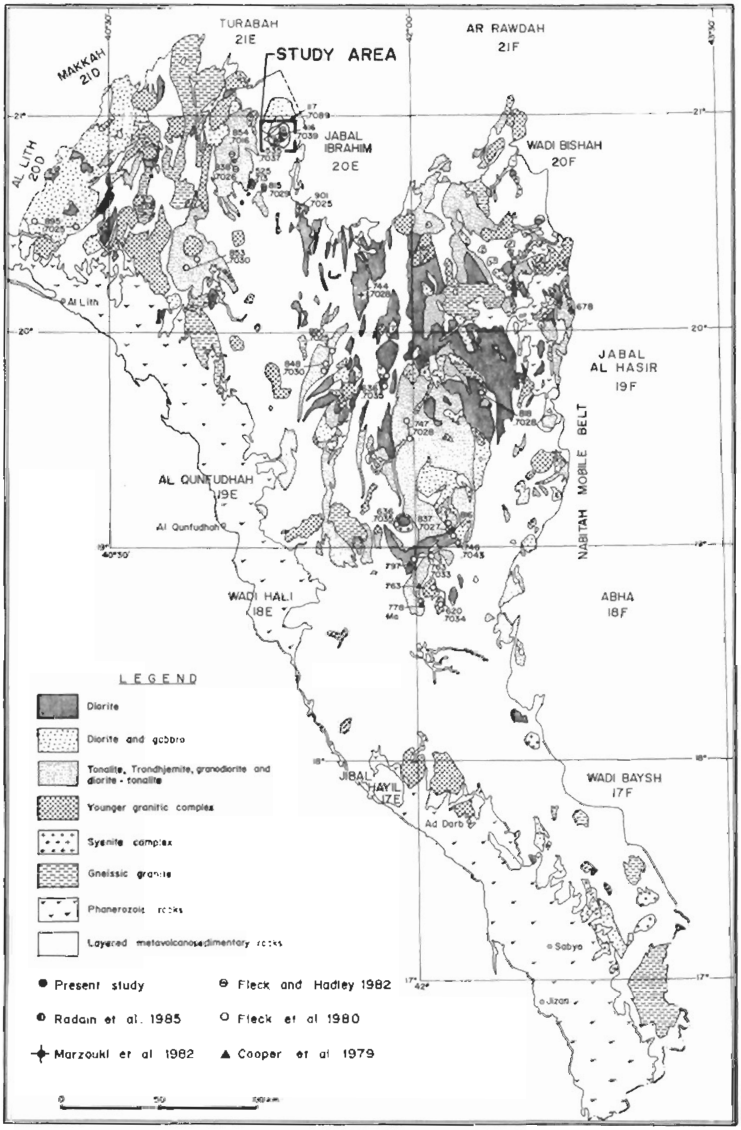

FIG. 2. Simplified geological map of the southern part of the Asir microplate showing Rb-Sr and U-Pb rock ages and $^{87}Sr/^{86}Sr$ initial ratios.

The felsic plutonic rocks of the Asir microplate have a wide spectrum of diorite-tonalite-trondhjemite, gabbro-diorite, granodiorite, granite and gneisses (Fig. 2). The geochronological studies (Cooper *et al.* 1979, Fleck *et al.* 1980, Radain and Nasseef 1982, Marzouki *et al.* 1982, Radain *et al.* 1986) indicate that the oldest subduction related volcanic rocks and related metasediments are intruded by plutonic rocks *i.e.*, diorite, tonalite-trondhjemite, and quartz diorite, apparently derived from destructive plate margins. In the Jabal Ibrahim quadrangle (20 E), the diorite-tonalites of the Bidah and the Thurrat plutons are dated by Rb-Sr whole rock isochrons at 901±37 and 744±22 Ma with initial $^{87}Sr/^{86}Sr$ ratios of 0.70246 and 0.70281, respectively (Marzouki *et al.* 1982). A large batholith and a small stock of tonalite-quartz diorite occurring in the western and westcentral parts of the present study area produced Rb-Sr ages of 854±10 and 815±13 Ma (2σ) with initial $^{87}Sr/^{86}Sr$ ratios of 0.70159 and 0.7029, respectively. An intracratonic biotite granite from the same area defined an apparent Rb/Sr isochron age of 552±20 Ma (2σ) with a high initial $^{87}Sr/^{86}Sr$ ratio of 0.7133 (Radain and Nasseef 1982, Radain *et al.* 1987). Fleck and Hadley (1982) reported a Rb-Sr age of 838±93 Ma with an initial $^{87}Sr/^{86}Sr$ ratio of 0.7026 for a tonalite-quartz diorite batholith from the Wadi Shuqub quadrangle. Whereas, Radain *et al.* (1987) reported an age of 854±10 Ma with an initial $^{87}Sr/^{86}Sr$ ratio of 0.70159±0.00004 for the same batholith. A quartz diorite from Wadi Ash Shaqah Ash Shamiyah yields an age of 853±72 Ma with an initial $^{87}Sr/^{86}Sr$ ratio of 0.7026 (Fleck *et al.* 1980).

The Rb-Sr age determinations made on quartz dioritic rocks from the Al Lith (20 D), Al Qunfudah (19 E), and Jabal Al Hasir (19 F) quadrangles (Fig. 2) (Fleck *et al.* 1980) range from 895 to 746 Ma with initial $^{87}Sr/^{86}Sr$ ratios varying from 0.7025 to 0.7043.

The U-Pb ages reported by Cooper *et al.* (1979), on subduction related plutonic rocks of the An Nimas batholith range from 837 to 763 Ma. The U-Pb age determined by the same author on the intracratonic Bishah red granite situated in the southcentral part of the Wadi Bishah quadrangle yielded an age of 678 Ma. This paper reports the geochronological and geochemical studies carried out on the subduction related and intracratonic felsic plutonic rocks of the Wadi Turabah ring complex, occurring in the northcentral part of the southern Asir microplate (Fig. 2).

Geology and Petrography

A simplified geological map of the area (Fig. 3) shows a prominent ring structure. Reconnaissance geologic mapping of the Wadi Shuqub quadrangle was done by Greene and Gonzalez (1980). They referred to the Wadi Turabah ring structure as a circular intrusive structure consisting of a syenite-trondhjemite complex with probably other rock types in the central part of the complex. More recently, Alwashe *et al.* (1984), and Divi *et al.* (1984), carried out detailed geological and structural studies of the Wadi Turabah area, respectively. The felsic plutonic rocks occurring within the ring structure range in composition from diorite-tonalite through granodiorite-granite. The felsic plutonic rocks of the ring structure are intruded into the volcanic-arc assemblage of layered metavolcanic and metasedimentary sequences of the Asir microplate (>900 Ma) (Fleck *et al.* 1980, Marzouki *et al.* 1982). Multiple plutonic activity obliterates the exact stratigraphic order of the rock units within the ring structure. The volcanic and plutonic rocks are interfingered with each other along strike and are metamorphosed to schist and gneisses, especially in the southwestern part of the ring structure.

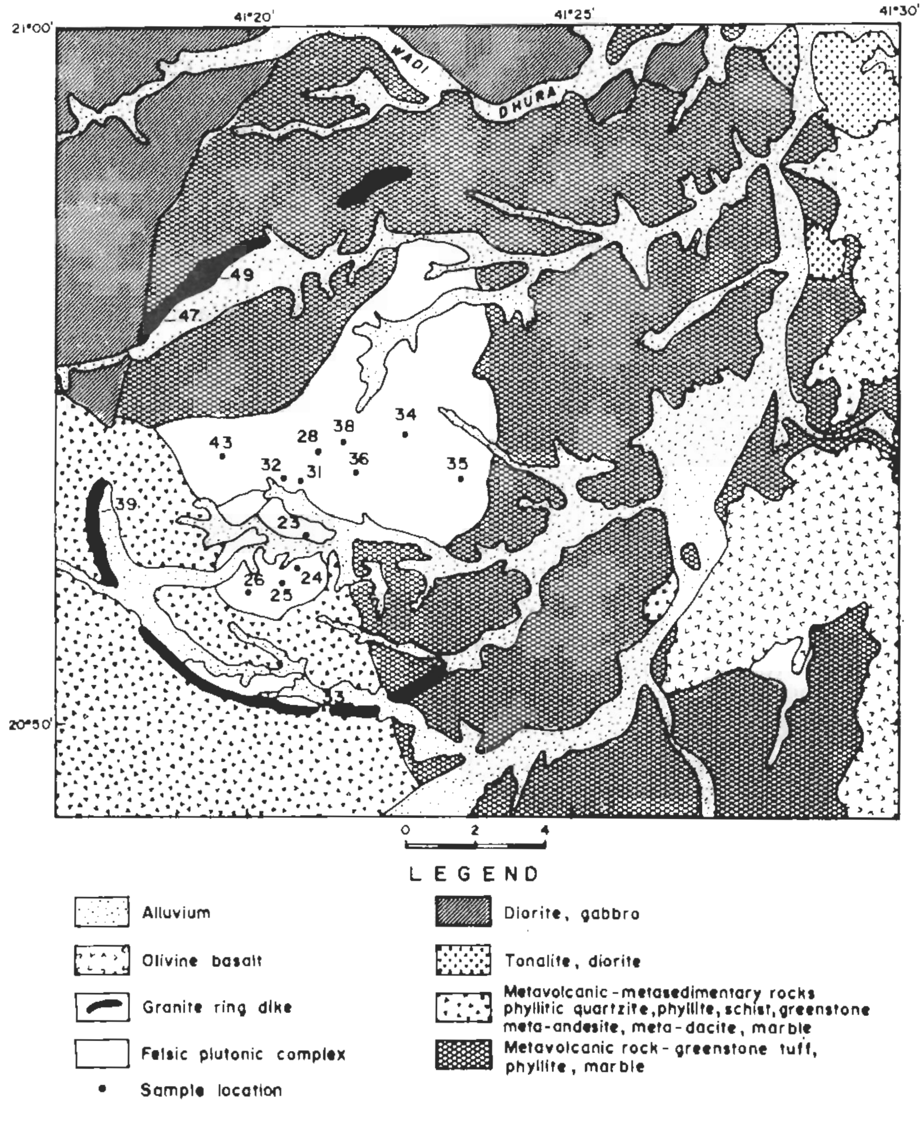

FIG. 3. Simplified geological map of the Wadi Turabah ring complex (after Greene and Gonzalez 1980).

Granodiorite-granite compositions dominate in the westcentral part of the ring structure with substantial amounts of gneissic tonalites in its south western part. The tonalite gneisses are composed mainly of sodic plagioclase (An_0-An_{30}) (50-55%), quartz (20-25%), biotite (10-20%), twined K-feldspar (0-5%), and hornblende (5-10%). The accessory minerals include magnetite, apatite, sphene, epidote, chlorite, and opaque minerals. Texturally, the rocks are medium to coarse-grained and show distinct gneissic texture. Foliation is well exhibited by dimensionally aligned biotite flakes and hornblende prisms. Plagioclase is highly saussuritized. However, remnants of albite and pericline twins are visible. Biotite is the most abundant ferromagnesian mineral, which also occurs in clusters with chlorite, K-feldspar, and magnetite. In places, the flakes of biotite are bent. Chlorite is derived chiefly from the hornblende. Two generations of quartz are present. The earlier generation is coarse, strained, and strongly undulase. The finer second generation occurs interstitially and has a replacement texture.

The gneissic granodiorites-granites which occur within the southwestern part of the ring structure are chiefly composed of crosshatched microcline perthite (50-60%), quartz (20-30%), oligoclase (An_{10}-An_{30}) (10-20%), orthoclase (5-10%), and biotite (5-10%). Apatite, sphene, magnetite, and zircon are accessory minerals. The large crystals of microcline perthite are characterized by the presence of rod, string, and replacement perthite. Quartz occurs as coarse grains with abundant cracks filled with white mica. Plagioclase is commonly sericitized. Biotite is the predominant mafic mineral and has inclusions of sphene, apatite, and zircon.

The massive diorite and granodiorite-granite suite rocks predominate within the eastcentral part of the ring structure. All rock units of the group are interfingered with each other. Sills of granite and granodiorite are interlayered with rocks of the volcano-sedimentary layered sequence. Xenoliths of the layered volcanic rocks of variable dimensions are found within the group of diorite and granodiorite-granite rocks. Diorite rock is composed of 60% of andesine (An_{30}-An_{40}), 20% of hornblende, 10% of biotite, 5% of chlorite and < 5% of quartz and other accessory minerals. Plagioclases have inclusions of apatite and iron ore. Hornblende is partly replaced by biotite and most of the biotite is altered to chlorite. Granodiorite-granite rocks are medium to coarse grained and composed of zoned plagioclase (An_{10}-An_{30}), (10-40%), quartz (20-35%), orthoclase (20-30%), biotite and hornblende (10-20%). Apatite, sphene, and magnetite are important accessories. Plagioclase is partially altered to white mica. Quartz is strained and has two generations.

The massive granitic rocks which form the semi-circular ring are generally coarse-grained of pinkish to grayish color. They crop out as discontinuous semi-circular ridges in the southern and western parts of the complex. They have sharp contacts and discordant relationship with the surrounding rocks. Structural (Divi *et al.* 1984) and age data (this study) suggest a post-tectonic emplacement. The granites are generally medium to coarse-grained and composed predominantly of microcline perthite (40-50%), K-feldspar (10-20%), plagioclase mostly albite (20-30%), and biotite (2-5%). Accessory minerals in the granites are hornblende, sphene, apatite, zircon, magnetite, and iron ore.

Analytical Methods

Major elements were determined by Phillips PW-1410 X-ray fluorescence spectrometry (XRF) using lithium tetraborate fusion. Na_2O and K_2O were determined by Turner Flame photometer, Model 510. MgO content was determined by atomic absorption using a Perking Elmer 305-B Model, and FeO by conventional chemical method.

Rb and Sr concentrations were determined by conventional X-ray fluorescence techniques (Pankhurst and O'Nions 1973). Sr-extraction was carried out using conventional sample-dissolution and standard ion exchange methods. All strontium isotopic ratios were measured on unspiked aliquots of the whole rock powders on a VG Isomass 54 E mass spectrometer with on-line data facilities in the Faculty of Earth Sciences, King Abdulaziz University (KAU), Jeddah. During the course of analyses, the NBS-987 Sr standard yielded a mean value of 0.710231 and a standard deviation of 0.00006. All strontium isotopic analyses are normalized to $^{87}Sr/^{86}Sr$ = 0.1194.

Rb/Sr isochrons were computed using the least-squares regression method of York (1969). The age calculations were made using a computer program of McSaveney (Faure 1977) which was modified at KAU to suit the HP-9845 B Desk top computer. The decay constant used for the Rb/Sr ages is Rb = $1.42 * 10^{-11}$/Y (Steiger and Jager 1977).

Geochemical Results

Major elements data, CIPW norms, and some chemical ratios are given in Tables 1 and 2. A chemical classification of Condie and Hunter (1976) is used to classify the granitoid complex. According to their classification, granitic or granodioritic rocks have a Na_2O/K_2O ratio of 2.0 or less, and tonalitic or trondhjemitic rocks have a Na_2O/K_2O ratio of 2.0 or more.

TABLE 1. Chemical analyses and CIPW norms of gneissic granodiorite-granite suite.

Sample	Tonalites		Gneissic granodiorites-granites					
	A 23	A 31	A 24	A 25	A 26	A 32	A 36	A 43
SiO_2	65.54	59.54	70.50	71.72	75.65	75.57	60.71	70.46
TiO_2	0.20	0.72	0.19	0.22	0.03	0.17	0.67	2.50
Al_2O_3	14.64	20.30	14.41	13.70	12.38	12.52	18.62	14.08
Fe_2O_3	3.49	2.26	1.61	1.41	0.41	0.54	1.90	0.93
FeO	3.16	11.69	0.90	1.04	0.40	0.57	1.54	1.22
MnO	0.12	0.06	0.04	0.04	0.02	0.02	0.57	0.04
MgO	2.10	1.23	0.46	0.45	0.80	0.32	1.00	0.40
CaO	7.00	4.50	1.47	2.02	0.49	1.12	3.50	1.90
Na_2O	2.56	5.73	4.04	3.72	3.64	3.20	5.69	3.88
K_2O	0.30	2.59	4.52	4.40	4.90	4.45	3.95	4.06

Table 1 (contd.).

Sample	Tonalites		Gneissic granodiorites-granites					
	A 23	A 31	A 24	A 25	A 26	A 32	A 36	A 43
P_2O_5	0.09	0.23	0.02	0.05	0.02	0.02	0.21	0.05
Rb (ppm)	5.7	13.9	52.5	53.0	70.9	48.8	17.1	49.7
Sr (ppm)	298.0	916.2	199.2	191.6	37.3	119.6	533.6	189.3
Na_2O/K_2O	8.53	2.21	0.89	0.84	0.74	0.72	1.44	0.96
Fe_2O_3 + FeO	6.65	3.95	2.51	2.45	0.81	1.11	3.44	2.15
K/Rb	437	1547	715	689	574	757	1917	678
CIPW norms								
q	32.02	5.46	26.37	28.97	33.79	37.55	4.13	27.98
c	–	0.43	0.25	–	0.25	0.47	–	–
or	1.79	15.48	27.21	26.32	29.32	26.64	23.73	24.11
ab	21.84	49.05	34.83	31.87	31.19	27.49	48.95	32.99
an	27.79	21.07	7.30	7.78	2.33	5.51	13.83	9.05
wo	2.76	–	–	0.85	–	–	1.01	–
en	5.27	3.10	1.17	1.13	2.02	0.81	2.53	1.00
fs	2.83	0.16	0.08	0.46	0.39	0.36	1.23	–
mt	5.10	3.31	2.38	2.07	0.60	0.79	2.80	–
hm	–	–	–	–	–	–	–	0.93
il	0.38	1.38	0.37	0.42	0.06	0.33	1.29	2.67
tn	–	–	–	–	–	–	–	0.06
ru	–	–	–	–	–	–	–	1.08
ap	0.21	0.55	0.05	0.12	0.05	0.05	0.51	0.12
DI	55.64	70.00	88.41	87.16	94.01	89.68	76.81	85.08

TABLE 2. Chemical analyses and CIPW norms of massive granodiorite-granite suite and granite ring dike.

	Diorite	Massive granodiorite-granite				Granite ring dike			
Sample No	A 34	A 13	A 28	A 38	A 41	A 33	A 39	A 47	A 49
SiO_2	55.60	72.86	75.52	76.29	62.22	64.17	73.83	75.58	75.16
TiO_2	1.45	0.11	0.06	0.06	0.84	0.39	0.11	0.50	0.25
Al_2O_3	18.42	13.50	12.52	12.28	15.86	18.49	13.46	12.38	13.46
Fe_2O_3	4.59	0.71	0.64	0.67	3.13	1.03	0.76	0.80	0.55
FeO	4.24	0.66	0.36	0.29	2.26	0.75	0.93	0.47	0.50
MnO	0.12	0.02	0.01	0.02	0.09	0.04	0.04	0.02	0.05
MgO	2.53	0.50	0.12	0.12	1.94	0.35	0.18	0.15	0.08
CaO	8.05	4.37	1.22	0.87	4.20	1.12	0.70	1.12	1.92
Na_2O	3.98	3.96	2.88	3.76	4.62	5.34	3.93	3.34	4.04
K_2O	0.96	3.50	5.45	4.60	2.95	6.29	4.90	4.73	4.70
P_2O_5	0.46	0.02	0.02	0.01	0.23	0.03	0.02	0.01	0.05
Rb (ppm)	14.7	74.70	55.7	130.9	69.3	28.1	79.9	42.4	52.6
Sr (ppm)	755.7	372.1	12.3	28.1	557.6	41.6	93.0	130.4	3.2
Na_2O/K_2O	4.15	1.13	0.53	0.82	1.57	0.85	0.80	0.70	0.86
Fe_2O_3 + FeO	8.83	1.37	5.39	0.96	1.00	1.78	1.69	1.27	1.05
K/Rb	542	389	812	292	353	1858	509	926	745
CIPW norms									

Table 2 (contd.).

	Diorite	Massive granodiorite-granite				Granite ring dike			
Sample No	A 34	A 13	A 28	A 38	A 41	A 33	A 39	A 47	A 49
q	9.78	28.87	35.74	35.43	14.09	6.33	30.41	35.92	30.25
c	–	–	–	–	–	0.95	0.47	–	–
or	5.65	20.64	32.60	27.47	17.73	37.93	29.29	28.20	26.52
ab	33.55	33.44	24.67	32.15	39.76	46.11	33.64	28.52	33.94
an	29.44	8.71	5.20	3.08	14.06	5.47	3.38	4.86	4.71
wo	3.07	5.34	0.33	0.51	2.32	–	–	0.28	1.96
en	6.28	1.24	0.30	0.30	4.91	0.89	0.45	0.38	0.20
fs	1.80	0.48	0.05	–	0.35	–	0.98	–	0.14
mt	6.63	1.03	0.94	0.83	4.61	1.45	1.11	0.13	0.79
hm	–	–	–	0.10	–	0.05	–	0.72	–
il	2.74	0.21	0.11	0.11	1.62	0.76	0.21	0.96	0.47
ap	1.08	0.05	0.05	0.02	0.55	0.07	0.05	0.02	0.02
DI	48.98	82.95	93.01	95.04	71.50	90.36	93.34	92.65	91.71

(a) Gneissic Granodiorite-Granite Suite

Eight samples were selected for major element analyses from this suite, two of them are gneissic tonalite and the remaining six are gneissic granodiorites-granites. When these two subgroups were compared, the gneissic tonalites were found to have higher Na_2O/K_2O ratios and concentrations of CaO, MgO, Al_2O_3, FeO(t), and lower SiO_2 and K_2O contents compared to the gneissic granodiorites-granites.

A ternary plot of AFM (Fig. 4) indicates calc-alkaline trend for the gneissic granodiorites-granites. The iron enrichment trend displayed by the gneissic tonalite may indicate hybrid nature.

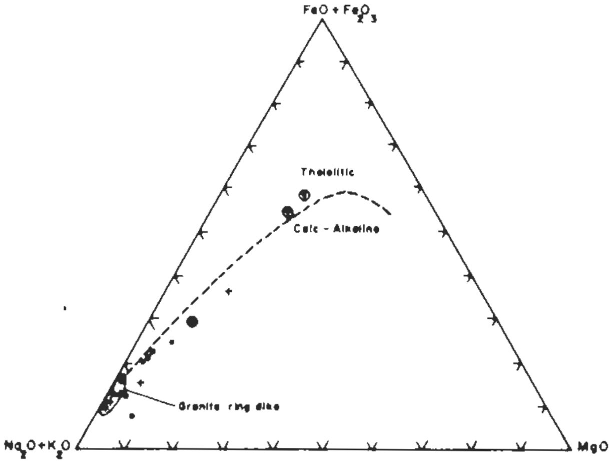

FIG. 4. AFM plot showing calc-alkaline trend. Circled point = Gneissic tonalite; Solid points = Gneissic granodiorite-granite; Circled crosses = Diorite; Crosses = Massive granodiorite-granite; Closed triangles = Ring dike granite.

On the ternary normative An-Ab-Or diagram (Fig. 5), gneissic granodiorite-granite rocks fall into the tonalite, trondhjemite, and granite fields, following the classification of O'Connor (1965). One of the tonalite samples indicates high An/Or ratio.

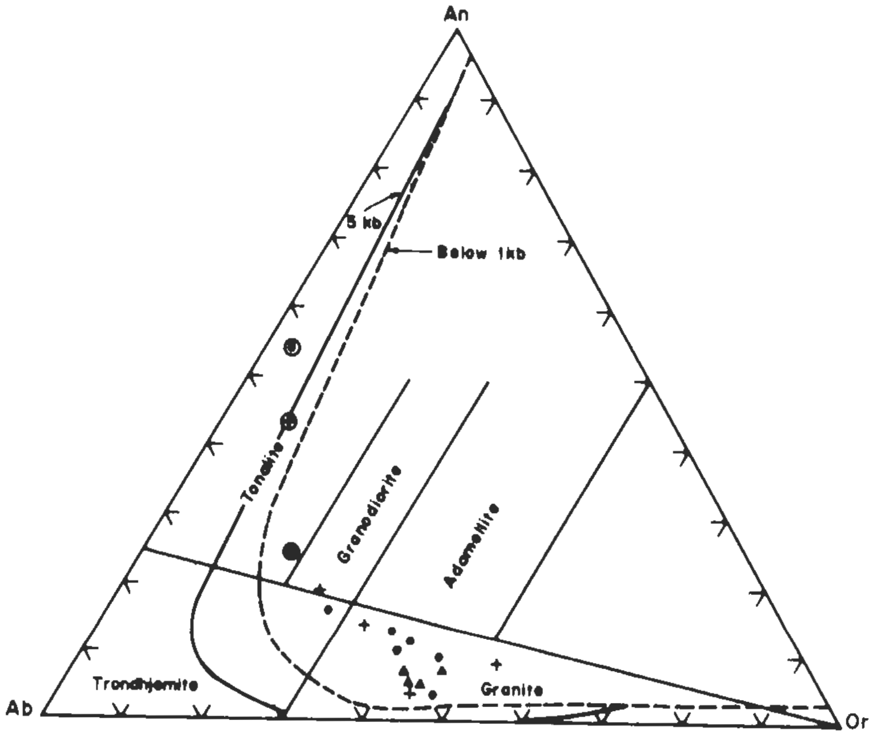

FIG. 5. An-Ab-Or ternary diagram. Petrochemical classification from O'Connor (1965), and broken and dashed curves are plagioclase boundaries as reported by Turner and Verhoogen (1960). Symbols as in Fig. 4.

The normative Q-Or-Ab diagram (Fig. 6) shows that the gneissic tonalite samples fall outside the low temperature trough and indicate crystallization from water saturated high temperature melts at a depth of about 10-16 km in the crust (Burnhan 1967). The gneissic granodiorites-granites plot in the low temperature trough (except sample A36) and indicate crystallization from a water undersaturated melt (2-3% H_2O) and a lower depth of about 4 km (Burnhan 1967). This variation indicates wide depth range in which GGGS rocks crystallized.

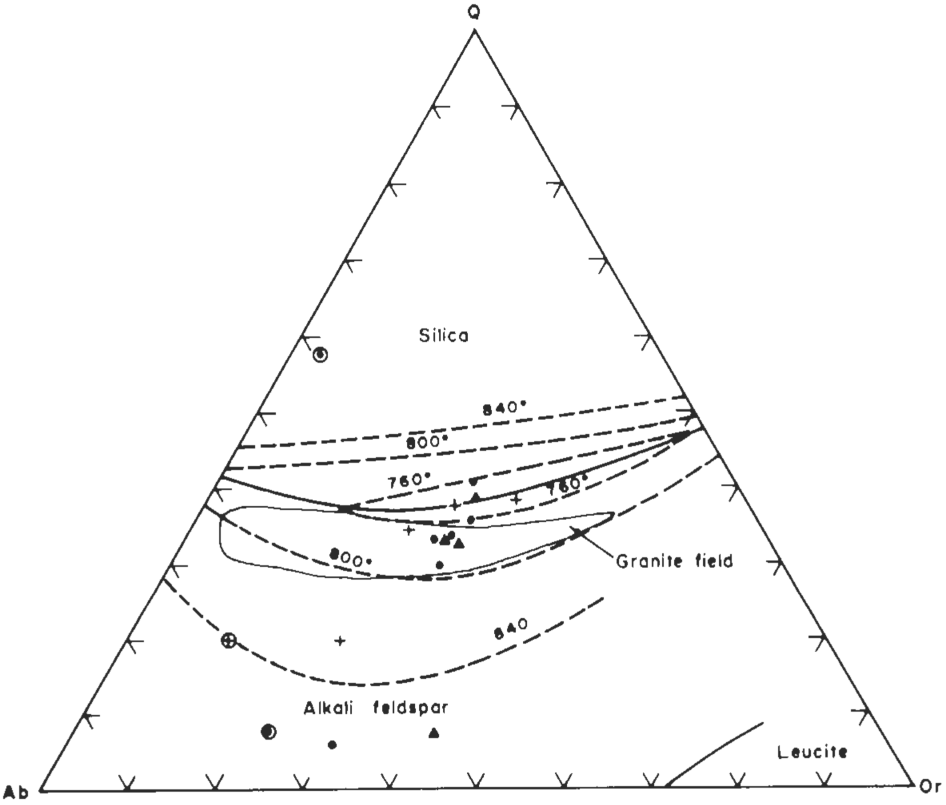

FIG. 6. Projection of the 1 Kb water pressure equilibrium diagram in the system $NaAlSi_3O_8$–$KAlSi_3O_8$–SiO_2 (after Tuttle and Bowen 1958). Granite field after Chayes reported by Turner and Verhoogen (1960). Symbols as in Fig. 4.

A semilog plot of SiO_2 VS K_2O % (Fig. 7) indicates very low concentration of K_2O (0.30%) for sample A23 of tonalite, which falls in the plagiogranite field. The distinguishing factor between oceanic plagiogranite and continental trondhjemite-tonalite associated with Phanerozoic orogenic belts is still an enigma (Coleman and Peterman 1975). The small number of samples preclude any concluding remarks regarding the nomenclature of this tonalite neither its genesis or affiliation. The gneissic granodiorites-granites fall within or near the boundary of continental granophyre.

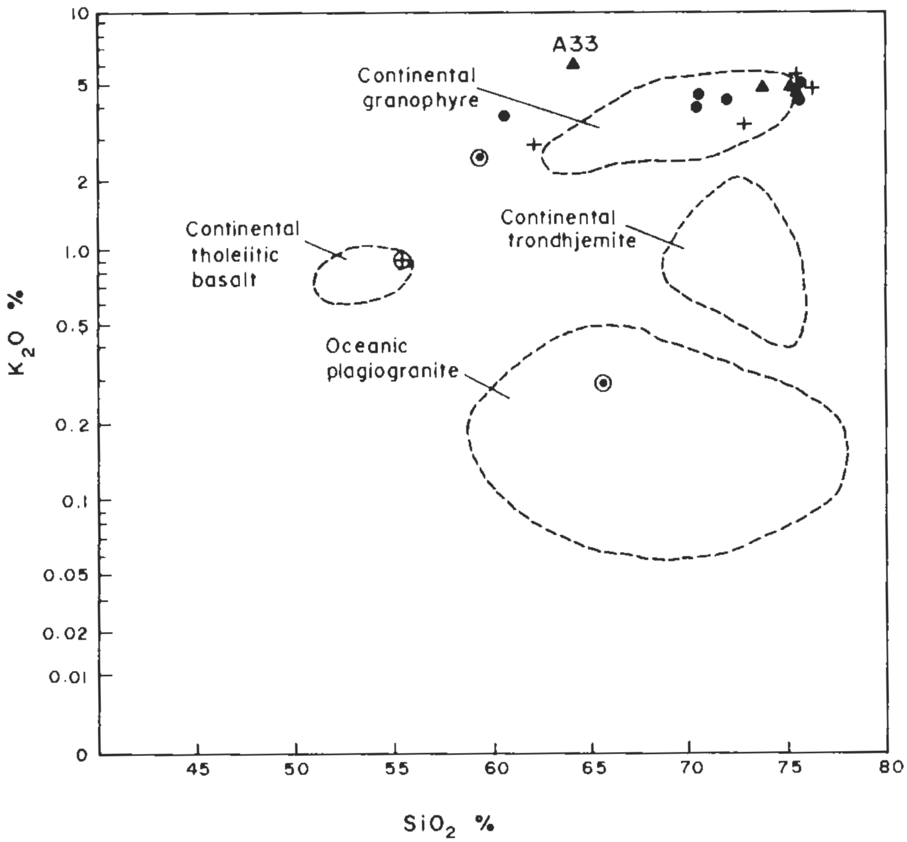

FIG. 7. A semilog plot of SiO_2 VS K_2O. The fields of other rock suites are shown by Coleman and Peterman (1975). Symbols as in Fig. 4.

The K/Rb ratios (Fig. 8) in the two gneissic tonalites indicate much variability (437-1547 ppm). The gneissic granodiorites-granites also display a significantly wide spread in K/Rb ratios, ranging from 574 to 1917 ppm (Table 1). The over all K/Rb values for the gneissic granodiorites-granites suite are higher than the crustal range (120-480, Taylor 1966, Shaw 1968). Hart and Aldrich (1967), Griffin and Murthy (1969) and Murthy and Griffin (1970) have suggested that the higher K/Rb liquids can be derived by partial melting of the upper mantle in which the contribution of plagioclase and hornblende melt is high.

A possible alternative explanation for the high K/Rb ratios can be derived from the studies of Sighinolfi (1971), Heier (1973), and Turner (1980) who have pointed out that both K and Rb contents decrease and K/Rb ratios increase in granulite facies rocks. The possible depletion mechanisms of these elements in granulite facies rocks

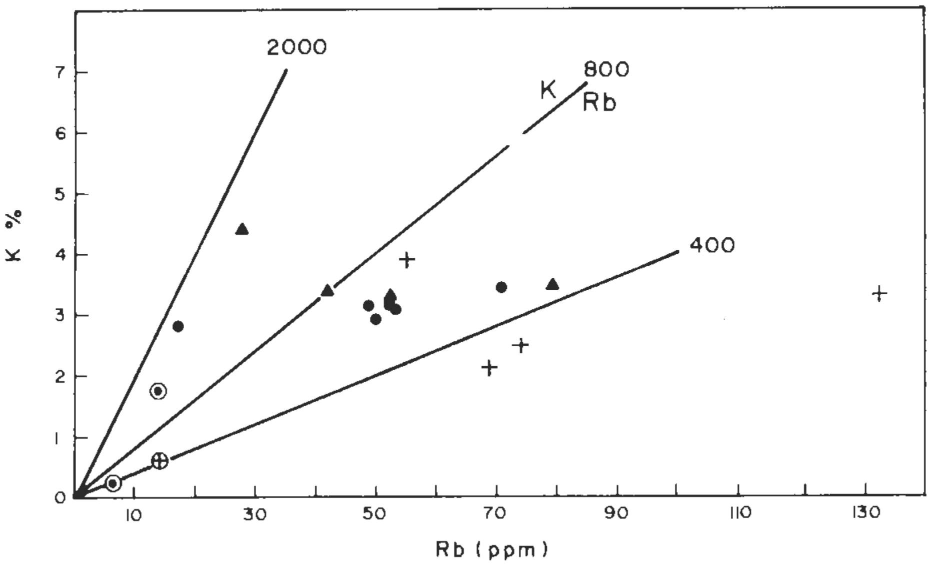

FIG. 8. K/Rb variation diagram. Symbols as in Fig. 4.

has been attributed to dehydration reactions and melting processes. However, geological studies of Greene and Gonzalez (1980) and Alwashe *et al.* (1984) reveal that the rocks of the ring complex are in the upper greens chist-lower amphibolite metamorphic facies. Thus, the absence of granulite facies conditions indicate that the rocks might have been derived from lower crust (granulitic rocks) or upper mantle source.

The oxides percentages are plotted against differentiation indices (Fig. 9) of Thornton and Tuttle (1960), DI = normative Q + Or + Ab, in this study. The DI values for the two gneissic tonalites are 56 and 70. In the gneissic granodiorites-granites it ranges from 76.81 to 94.01. The MgO, CaO, MnO, and FeO(t) contents decrease with increase of DI. In contrast, K_2O and Na_2O rise with the DI increase. With rise in DI, the gneissic granodiorites-granites show an increase in SiO_2 and K_2O and a decrease in Al_2O_3, FeO(t), MgO, CaO, TiO_2 and P_2O_5. A roughly linear trend is observed for Na_2O and MnO. The well correlated increasing and decreasing trends in oxides suggest that the gneissic granodiorites-granites are probably cogenetic products of a magmatic differentiation process.

(b) Massive Granodiorite-Granite Suite

Five samples were analyzed from this suite, one of the samples is diorite and the others are granodiorites-granites. The diorite exhibits its typical chemical characteristics. Some of the salient features of the diorite are high Al_2O_3, CaO, MgO, FeO(t), low content of K_2O and intermediate silica value (Table 2).

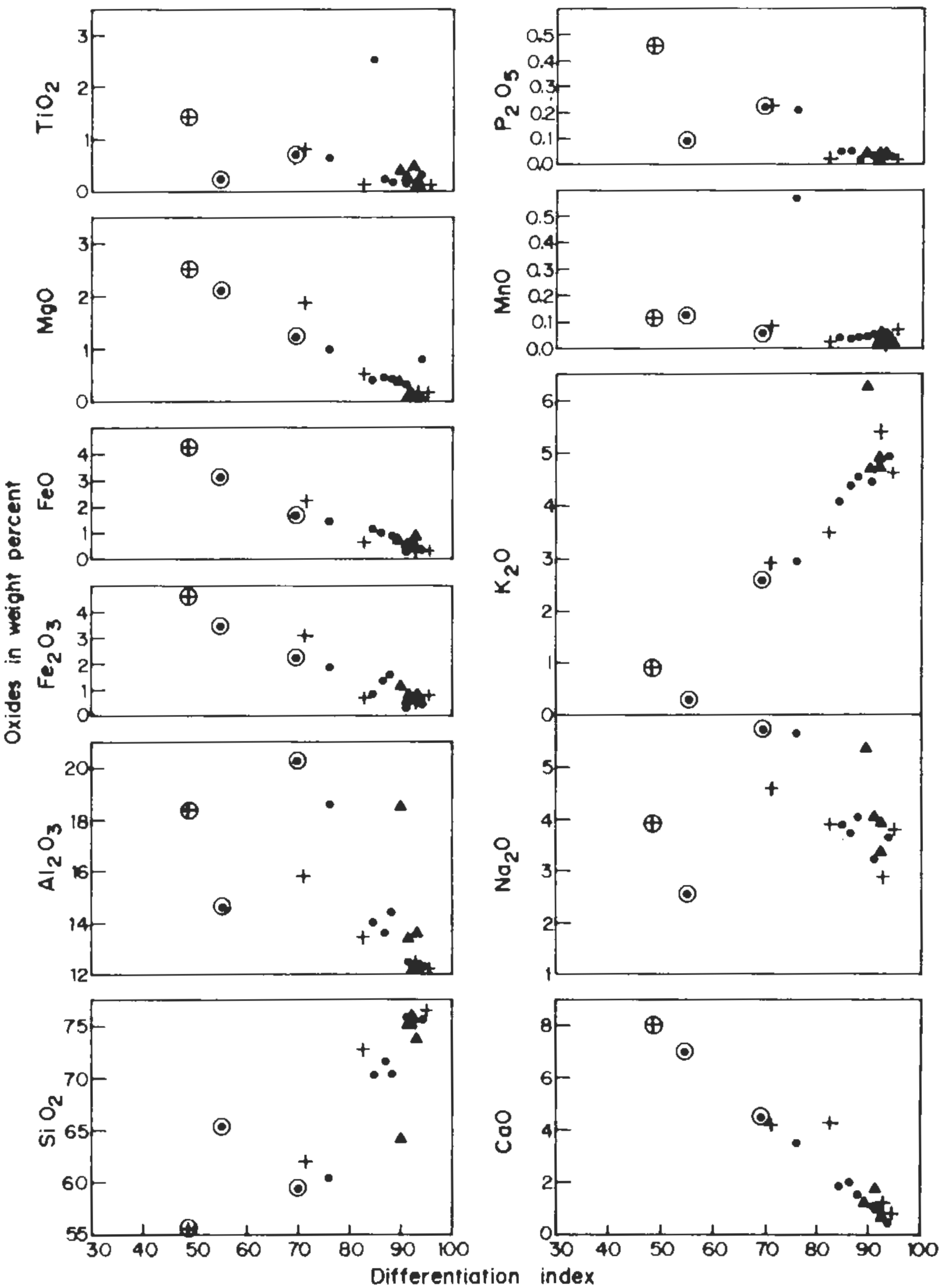

FIG. 9. Plots of major oxides against differentiation index (Di = normative Q+Or+Ab). Symbols as in Fig. 4.

The AFM diagram (Fig. 4) indicates a calc-alkaline trend for granodiorites-granites. The diorite sample with Fe enrichment most probably represents hybrid rock.

In the An-Ab-Or diagram (Fig. 5), all samples of the gneissic granodiorites-granites fall in the two feldspar field with low water pressure (<1 Kb) and indicate shallow levels of magma crystallization. The dioritic rock falls on the boundary of the one feldspar field, indicating high pressure and moderate temperature of formation with deeper level of magma crystallization.

In the ternary minimum system Q-Or-Ab (Fig. 6), the granodiorites-granites fall both inside and outside the low temperature trough. A high temperature and water saturated conditions at the initial stages followed by low temperature and pressure are suggested by the dispersion of the samples. The diorite sample fall in the high temperature field.

A semilog plot of SiO_2 VS K_2O (Fig. 7) for diorite shows the affinity with continental tholeiitic basalt. On the other hand, granodiorites-granites fall within or close to the boundary of continental granophyres shown by Coleman and Peterman (1975).

The K/Rb ratio (Fig. 8) for the massive diorite and granodiorites-granites suite varies from normal values (292, 353, 389) or crustal range to values >480 (542, 812). This bimodal distribution of K/Rb indicates that the diorite and granodiorites-granites suite is likely to have been derived by partial melting of different parent materials of lower and upper crustal compositions.

The oxides VS DI are plotted in Fig. 9. The diorite and granodiorites-granites rocks indicate the decrease of Al_2O_3, FeO(t), MgO, TiO, MnO, and P_2O_5 and the increase of SiO_2 and K_2O with the increase of DI values. The trend of Na_2O is roughly linear. The DI ranges from 49 to 93. These positive and negative trends with DI suggest an origin involving a magmatic differentiation process.

(c) Ring Dike Granites

Significant variations are not found in chemical composition of granites. Alkali abundances do not vary much, the Na_2O/K_2O ratios range from 0.71 to 0.86. Silica contents vary between 73.83% and 75.58% except sample A 33, which has moderately low silica content of 64.17%. The MgO, MnO, TiO_2, and $FeO+Fe_2O_3$ concentrations are low.

The narrow distribution pattern of the granites on the AFM diagram (Fig. 4) indicates constant ferromagnesium and alkali contents of the magma.

On the An-Ab-Or ternary diagram (Fig. 5), the granites fall well inside the two feldspar field. The low dispersion pattern reflects constant pressure and temperature conditions during crystallization of the magma.

The plot of Q-Ab-Or (Fig. 6) shows that all granites (except one) fall well inside the low temperature trough and indicates crystallization from a shallow seated water undersaturated melt.

On the semilog plot of SiO_2 VS K_2O (Fig. 7), all granites (except one) fall on the higher SiO_2 content boundary of the continental granophyre field of Coleman and Peterman (1975).

The youngest ring dike granites show high and wide variation of K/Rb ratios (Fig. 8), ranging from 509 to 1858. This type of wide variation is observed only in the granulite facies rocks (Green *et al.* 1972, Tarney and Windley 1977). However, some young granites within the granulite facies areas have displayed high K/Rb ratios and they have indicated their derivation by partial melting of rocks already in granulite facies conditions (Heier and Brunfelt 1970). Thus, it might be inferred that the ring dike granite is a product of partial melting of the crustal rocks which were having the characteristics of granulite facies rocks.

The percentages of oxides do not show any striking variation trend against DI (Fig. 9). The value of DI ranges from 90 to 95 which suggests highly developed stage of evolution. Such low variations also suggest that the granites might have crystallized from a ternary minimum composition in the system, SiO_2-$NaAlSiO_4$-$KAlSiO_4$.

Rb/Sr Isochron Plots

(a) Gneissic Granodiorite-Granite Suite

Six samples from the southwestern part of the Wadi Turabah ring structure were selected for Rb-Sr isochron. A six point errochron defines an apparent age of 535±11 Ma, and an initial $^{87}Sr/^{86}Sr$ ratio of 0.7037±0.00006, MSWD = 6.6 (Fig. 10, Table 3).

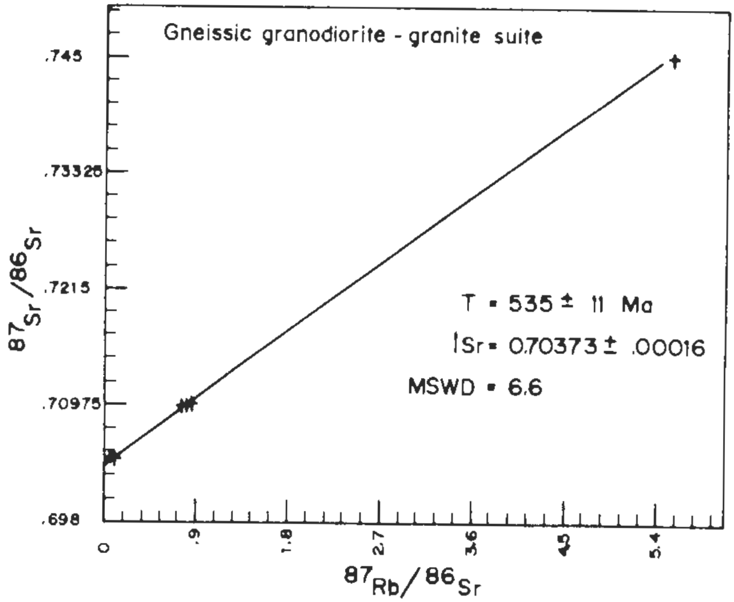

FIG. 10. $^{87}Rb/^{86}Sr$ VS $^{87}Sr/^{86}Sr$ errochron plot. Age and initial $^{87}Sr/^{86}Sr$ ratio are given at 2 sigma level.

(b) Massive Granodiorites-Granites Suite

Five samples were selected from the westcentral and central parts of the Wadi Turabah circular intrusive structure. Four of them are granodiorites-granites and remaining one is diorite. A five point isochron produced an errochron which corresponds to an age of 416±9 Ma, and an initial $^{87}Sr/^{86}Sr$ ratio of 0.704±0.0002, MSWD = 9.01 (Fig. 11, Table 3). If we drop the petrochemically different diorite sample from the regression, four points define an isochron corresponding to an age of 419±0.2 Ma (2σ), with an initial $^{87}Sr/^{86}Sr$ ratio of 0.7038±0.00002, MSWD = 2.0.

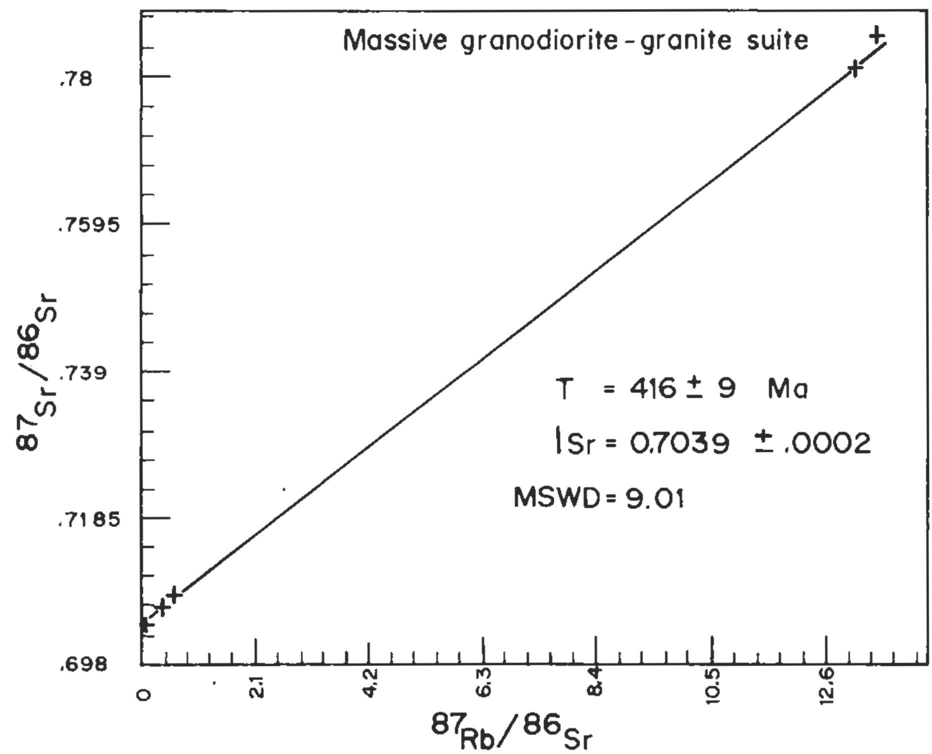

FIG. 11. $^{87}Rb/^{86}Sr$ VS $^{87}Sr/^{86}Sr$ isochron plot. Age and initial $^{87}Sr/^{86}Sr$ ratio are given at 2 sigma level.

(c) Ring Dike Granite

Four granite samples were selected from the granite ring dike at different places. A four point samples isochron defines an apparent age of 117±0.4 Ma and an initial $^{87}Sr/^{86}Sr$ ratio of 0.70894±0.00015; MSWD = 0.01 (Fig. 12, Table 3).

TABLE 3. Rb-Sr whole rock data for the Wadi Turabah felsic plutonic ring complex.

Sample Number	Rb (ppm)	Sr (ppm)	Rb/Sr (Wt.)	$^{87}Rb/^{86}Sr \pm 2\sigma$ (atomic)	$^{87}Sr/^{86}Sr \pm 2\sigma$ (atomic)
Gneissic granodiorite-granite suite					
A-23	5.7	298.0	0.0191	0.0552±.0011	.704395±.080
A-24	52.5	199.2	0.2636	0.7629±.0152	.709547±.058
A-25	53.0	191.6	0.2768	0.8009±.0160	.709723±.074
A-26	70.9	37.3	1.9010	5.5205±.0110	.745368±.050
A-36	17.1	533.6	0.0321	0.0930±.0018	.704288±.050
A-43	49.7	189.3	0.2625	0.7596±.0152	.709688±.038
Massive granodiorite-granite suite					
A-13	74.7	372.1	0.2009	0.5812±.0116	.707657±.036
A-28	55.7	12.3	4.5190	13.1685±.2634	.780848±.100
A-34	14.7	755.7	0.0194	0.0562±.0012	.703482±.108
A-41	69.3	557.6	0.1242	0.3594±.0072	.705985±.044
A-38	130.9	28.1	4.6598	13.5092±.2702	.784912±.130
Granite ring dike					
A-33	28.1	41.6	0.6750	1.9539±.0390	.712095±.062
A-39	79.9	93.0	0.8602	2.4902±.0498	.712876±.058
A-47	42.4	130.4	0.3253	0.9416±.0188	.710785±.100
A-49	52.6	3.2	17.0440	49.7180±.9944	.791382±.076

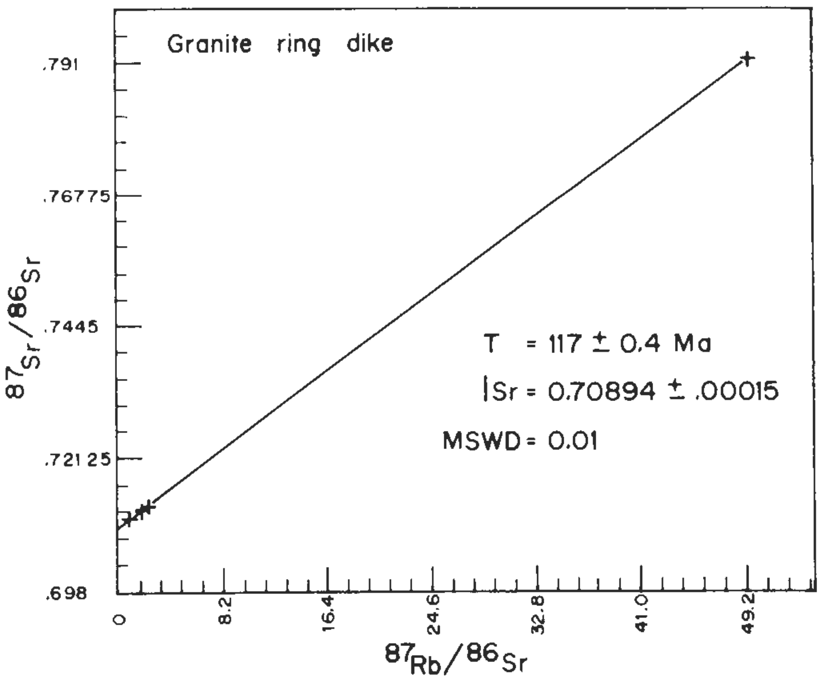

FIG. 12. $^{87}Rb/^{86}Sr$ VS $^{87}Sr/^{86}Sr$ isochron plot. Age and initial $^{87}Sr/^{86}Sr$ ratio are given at 2 sigma level.

Discussion and Conclusions

Final isotopic age data (Table 4) together with geochemical studies, provide some clues on the sequence of tectonic and geochemical evolution of the area. The evolution of the crust started with subduction related volcanic magmatism and related sedimentation (Baish and Bahah groups of Schmidt *et al.* 1973). Geochemical data reported by Jackaman (1972) indicates tholeiitic trend for this volcanic magmatism. The Baish group was referred to as a "Juvenile oceanic island arc" deposited in a subaqueous environment with a chemical resemblance to the flow rocks of an "island arc tholeiitic series" (Greenwood *et al.* 1976, Jakes and Gill 1970). Recent studies show that the Baish and Bahah groups have no stratigraphic break. These rock groups have inter-tonguing relationships (Greenwood *et al.* 1980, Ramsay *et al.* 1981, Riofinex 1977, Alwashe *et al.* 1984).

TABLE. 4. Final regression data for felsic plutonic rocks of Wadi Turabah ring complex, central Arabian Shield.

Rock suite	Age (Ma)	Initial $^{87}Sr/^{86}Sr \pm 2\sigma$	MSWD	No. of points	Models York (1969)
Gneissic granodiorite-granite	535±11	0.70373±.00016	6.6	6	II
Massive granodiorite-granite	416±9	0.70390±.0002	9.0	5	II
Granite ring dike	117±.4	0.70894±.00015	0.01	4	I

The multiple orogenic events from 960 Ma to 600 Ma (described as the Aqiq, Ranyah, and Yafikh orogenies by Greenwood *et al.* 1976) are reflected in the form of multiple deformation and plutonic intrusions within the northerly trending tectonic belt of layered rocks that were metamorphosed under upper greenschist and lower amphibolite facies conditions. The oldest dated rock reported in this paper is 535±11 Ma. However, a six point isochron for the Wadi Shuqub tonalite-quartz diorite stock occurring in the south central part of the Wadi Shuqub quadrangle (Fig. 3) defines an age of 815±27 Ma and an initial ratio of 0.70292±10 (2σM), MSWD = 1.80. An age of 854±10 Ma is reported for tonalite-quartz diorite rock, collected along the Hijaz Highway (Fig. 2), the initial $^{87}Sr/^{86}Sr$ ratio for this suite is very low 0.7015±8 (2σM). The intracratonic intrusive biotite granite from the Gabalat area, situated in the central part of the Jabal Ibrahim (20 E) quadrangle (Fig. 2) is dated at 552±20 Ma, and an initial $^{87}Sr/^{86}Sr$ ratio of 0.71321±0.003, MSWD = 4.47. All the above ages are reported by Radain *et al.* (1987). Fleck and Hadley (1982) also reported a Rb-Sr isochron age of 838±93 Ma and an initial $^{87}Sr/^{86}Sr$ ratio of 0.7026 for the large batholith of tonalite quartz diorite occurring along the Hijaz Highway (Fig. 2) in the Jabal Ibrahim quadrangle, where Radain *et al.* (1987) reported an age of 854±10 Ma.

The low initial $^{87}Sr/^{86}Sr$ ratios indicated by the oldest tonalite-quartz diorite rocks indicate direct derivation from the mantle or lower crust. The Gabalat granite with high initial $^{87}Sr/^{86}Sr$ ratio of 0.71321±0.003, indicates its derivation from the partial or complete melting of highly evolved crust. The undisturbed low initial $^{87}Sr/^{86}Sr$ ratio indicate stability in the western part of the Wadi Shuqub quadrangle. In contrast, the rock units of the Central and Eastern parts of the quadrangle are highly disturbed by younger acid igneous activities, especially in the Wadi Turabah ring structure.

Greene and Gonzalez (1980) referred to plutonic rocks occurring within the ring structure as syenite-trondhjemite complex. Brown (cited from Greene and Gonzalez 1980) collected samples from the southern part of the Wadi Turabah ring structure, where the dominant rock type is tonalite and granite-granodiorite gneisses, and reported an age of 550 Ma, without reporting the initial $^{87}Sr/^{86}Sr$ ratio and MSWD. In this study, a six point errochron from the same locality defined an apparent age of 535±11 Ma, and an initial $^{87}Sr/^{86}Sr$ ratio of 0.7037±0.00016, with a higher MSWD of 6.6 (Fig. 10). When highly altered samples of one tonalite and one granodiorite were rejected from the regression, an excellent isochron of four points was produced for gneissic granites, which corresponds to an age of 528±2 Ma with an initial $^{87}Sr/^{86}Sr$ ratio of 0.7038±.0001; MSWD = 0.0002. Thus, the intracratonic intrusion of granodiorites-granites composition at about 528 Ma into the tonalite, metavolcanic and metasedimentary rocks, succeeded by effects of deformation and metamorphism during the Pan-African orogeny might have led to partial or complete resetting of the Rb-Sr system in the older felsic plutonic units. The presence of older tonalite and other plutonic rocks within the ring structure cannot be ruled out. However, samples collected in this study indicate that the multideformation and metamorphic histories might have obliterated the older plutonic rocks at least in this part of the area and resetted with the younger intrusive rock of granodiorite-granite compositions. Thus, we can consider the 535±11 Ma date on the tonalite and granites-granodiorites as a mixed age of plutonism, metamorphism, and deformation, to which the rock has been subjected after the closing of the Rb-Sr whole rock systematics. However, there are many cases of "reset" for the Rb-Sr whole rock system in the literature. A geological terrane having experienced polyphase tectono-metamorphism is always prone to open system behavior, that is, diffusion of radiogenic ^{87}Sr into Common Strontium of the adjacent or intruded rock at the time of metamorphism. The loss of Rb or gain of Sr or *vice versa* may also prevail at the same time (Roddick and Compston 1977, Priem *et al.* 1978, Gale *et al.* 1979, Field and Raheim 1979, Beckinsale *et al.* 1980, Cameron *et al.* 1981, Feiko Kalsbeek 1981, Smalley *et al.* 1983, Wickman *et al.* 1983).

The structural studies carried out by Divi *et al.* (1984), indicate that the gneissic granites have multideformational and metamorphic histories. The absence of older plutonic rocks ages within the studied area may indicate that severe tectono-thermal events have led to open system behavior. Such behavior is reported by Black *et al.* (1979) who have described detailed multideformation and metamorphic effects resetting Rb/Sr whole rock isochron systems in the Georgetown Inlier of north Queensland, Australia.

The next episode of cratonal development in the Wadi Turabah ring structure involves the intrusion of younger granodiorite-granite rocks associated with diorite in the central and western parts of the ring structure. In these areas, it is intruded into the older units of its own clan and metavolcano-sedimentary rocks of Baish and Bahah groups. The age obtained from this suite is 416±9 Ma. (Fig. 11). A combined regression of diorite and granodiorites-granites indicates genetically related history.

The last phase of plutonic igneous activity in the form of the granite ring dike is attributed to the cauldron subsidence model (Greene and Gonzalez 1980). However, a Hertzian quasi-oval fracture model (Bahat 1980) suggested by Divi *et al.* (1984) for the Wadi Turabah ring complex attains much attention. The complex history of evolution of the area, indicated by multiple igneous activity, polyphase deformation, and metamorphism may be reflected in the form of Hertzian fractures at depths, followed by horizontal and vertical tension and lastly the development of quasi-oval fractures and intrusion of highly differentiated magma of ternary minimum composition (SiO_2-$NaAlSiO_4$-$KAlSiO_4$). The apparent age obtained from this granite ring dike is about 117±0.4 Ma, which is the lowest plutonic activity reported from the Arabian shield. However, this age of plutonic activity is well documented in the Northeast Sudan and Eastern Desert of Egypt (Hashad and El Reedy 1979). The high initial $^{87}Sr/^{86}Sr$ ratio of 0.7089±0.00015 (2σ) is well above expected values from the contemporaneous mantle (initial $^{87}Sr/^{86}Sr$ C.0.703) and indicates crustal source origin. The low spread in $^{87}Sr/^{86}Sr$ ratios and the number of samples, prompt further study of the area. The homogeneous granitic dike has discordant relationship with all deformational structures and supports younger age (Divi *et al.* 1984).

References

Alwashe, M.A., Divi, S. R. and **Groen, C.** (1984) *Geological map of Wadi Turabah-Wadi Dhura area, Central Arabian Shield*, Map Fac. Earth. Sci., King Abdulaziz University.

Bahat, D. (1980) A Hertzian quasi-oval fracture model for ring complex, *J. Geol.* **88:** 271-284.

Beckinsale, R.D., Gale, N.H., Pankhurst, R.J., MacFarlane, A., Crow, M.J., Arthurs, J.W. and **Wilkinson, A.F.** (1980) Discordant Rb-Sr and Pb-Pb whole rock isochron ages for the Archaean basement of Sierra Leone, *Precambrian Res.* **13:** 63-76.

Black, L.P., Bell, T.H., Rubenach, M.J. and **Withnall, I.W.** (1979) Geochronology of discrete structural-metamorphic events in a multiply deformed Precambrian terrain, *Tectonophysics* **54:** 103-137.

Burnhan, C.W. (1967) Hydrothermal fluids at the magmatic stage, *In:* **Barnes, H.L. (Ed.),** *Geochemistry of hydrothermal ore deposits*, Holt, Rinehart and Winston, New York, 670 p.

Cameron, M., Collerson, K.D., Compston, W. and **Morton, R.** (1981) The statistical analysis and interpretation of imperfectly-fitted Rb-Sr isochrons from polymetamorphic terrains. *Geochim. Cosmochim Acta.* **45:** 1087-1097.

Camp, V.E. (1984) Island arcs and their role in the evolution of the western Arabian Shield, *Bull. Geol. Soc. Am.* **95:** 913-921.

Coleman, R.G. and **Peterman, Z.E.** (1975) Oceanic plagiogranite, *J. Geophys. Res.* **80:** 1099-1108.

Condie, K.C. and **Hunter, D.R.** (1976) Trace element geochemistry of Archean granitic rocks from the Barberton region, South Africa, *Earth Planet. Sci. Lett.* **29:** 389-400.

Cooper, J.A., Stacey, J.S., Stoeser, D.B. and **Fleck, R.J.** (1979) An evaluation of the zircon method of isotopic dating in the southern Arabian craton, *Contrib. Mineral. Petrol.* **65:** 429-439.

Divi, S.R., Alwashe, M., Basahel, A.N. and **Groen, C.** (1984) Deformational structures within and outside a ring structure, Wadi Turabah, Central Arabian Shield, *Fac. Earth Sci., King Abdulaziz Univ., Bull.* **6:** 397-407.

Earhart, R.L. and **Mawad, M.M.** (1970) Geology and mineral evaluation of the Wadi Bidah district, Southern Hijaz quadrangle, Kingdom of Saudi Arabia. *U.S. Geol. Surv., Saudi Arabian Proj., Rept.* **119,** 100 p.

Faure, G. (1977) *Principles of Isotope Geology,* John Wiley and Sons, New York, pp. 425-436.

Field, D. and **Raheim, A.** (1979) A geologically meaningless Rb-Sr total rock isochron, *Nature* **282:** 497-499.

Fleck, R.J., Greenwood, W.R., Hadley, D.G., Anderson, R.E. and **Schmidt, D.L.** (1980) Age and evolution of the southern part of the Arabian Shield, *Inst. Appl. Geol. (Jeddah), Bull.* **3**(3): 1-17.

Fleck, R.J. and **Hadley, D.G.** (1982) Ages and strontium initial ratios of plutonic rocks in a transect of the Arabian Shield. *U.S. Geol. Surv., Saudi Arabian Proj., Rept.* **USGS-OF-03-38,** 43 p.

Gale, N.H., Beckinsale, R.D. and **Wadge, A.J.** (1979) Rb-Sr whole rock dating of acid rocks, *Geochemical Jour.* **13:** 27-29.

Gonzalez, L. (1973) Geologic map and sections of the Jabal Ann quadrangle, Kingdom of Saudi Arabia, *Saudi Arabian Dir. Gen. Miner. Resour., Geol. Map* **GM-2.**

Green, T.H., Brunfelt, A.O. and **Heier, K.S.** (1972) Rare-earth element distribution and K/Rb ratios in granulites, mangerites and anorthosites, Lofoten-Vesteraalen, Norway, *Geochim. Cosmochim. Acta.* **36:** 241-257.

Greene, R.C. and **Gonzalez, L.** (1980) Reconnaissance geology of the Wadi Shuqub quadrangle, Sheet 20/41 A, Kingdom of Saudi Arabia. *Saudi Arabian Dir. Gen. Miner. Resour., Geol. Map* **GM-54.**

Greenwood, W.R. (1975) Geology of the Al-Aqiq quadrangle, Kingdom of Saudi Arabia. *Saudi Arabian Dir. Gen. Miner. Resour., Geol. Map* **GM-23.**

Greenwood, W.R., Anderson, R.E., Fleck, R.J. and **Roberts, R.J.** (1980) Precambrian geologic history and plate tectonic evolution of the Arabian Shield, *Saudi Arabian Dir. Gen. Miner. Resour., Bull.* **24,** 35 p.

Greenwood, W.R. and **Brown, G.F.** (1973) Petrology and chemical analyses of selected plutonic rocks from the Arabian Shield, Kingdom of Saudi Arabia, *Saudi Arabian Dir. Gen. Miner. Resour., Bull.* **9,** 9 p.

Greenwood, W.R., Hadley, D.G., Anderson, R.E., Fleck, R.J. and **Schmidt, D.L.** (1976) Late Proterozoic cratonization in southwestern Saudi Arabia, *R. Soc. Lond. Phil. Trans.* **A280** : 517-527.

Greenwood, W.R., Stoeser, D.B., Fleck, R.J. and **Stacy, J.S.** (1982) Late Proterozoic island-arc complexes and tectonic belts in the southern part of the Arabian Shield, Kingdom of Saudi Arabia. *Saudi Arabian Deputy Ministry for Mineral Resources Open-File Rept.* **USGS-OF-02-8,** 46 p.

Griffin, W.L. and **Murthy, V.R.** (1969) Distribution of K, Rb, Sr and Ba in some minerals relevant to basalt genesis, *Geochim. Cosmochim. Acta* **33:** 1389-1414.

Hadley, D.G. and **Schmidt, D.L.** (1980) Proterozoic sedimentry rocks and basins of the Saudi Arabian Shield and their evolution, *Inst. Appl. Geol. (Jeddah), Bull.* **3**(4): 26-50.

Hart, S.R. and **Aldrich, L.T.** (1967) Fractionation of potassium/rubidium by amphiboles: Implications regarding mantle composition, *Science* **155:** 325-327.

Hashad, A.H. and **El-Reedy, M.W.M.** (1979) Geochronology of the anorogenic alkalic rocks, South Eastern Desert, Egypt, *Egypt. Geol. Surv. Annals,* **IX:** 81-101.

Heier, K.S. (1973) Geochemistry of granulite facies rocks and problems of their origin, *R. Soc. Lond. Phil. Trans.* **A273:** 429-442.

Heier, K.S. and **Brunfelt, A.O.** (1970) Concentration of Cs in high grade metamorphic rocks, *Earth Planet. Sci. Lett.* **9:** 416-420.

Jackaman, B. (1972) Genetic and environmental factors controlling the formation of the massive sulphide deposits of Wadi Bidah and Wadi Wassat, Saudi Arabia, *Saudi Arabian Dir. Gen. Miner. Resour., Tech. Record* **1972-1,** 243 p.

Jakes, P. and **Gill, J.** (1970) Rare earth elements and the island arc tholeiitic series, *Earth Planet. Sci. Lett.* **9:** 17-28.

Kalsbeek, F. (1981) The northward extent of the Archean basement of Greenland – A review of Rb-Sr whole rock ages, *Precambrian Res.* **14:** 203-219.

Marzouki, F.M.H., Jackson, N.J., Ramsay, C.R. and **Darbyshire, D.P. E.** (1982) Composition, age and origin of two Proterozoic diorite-tonalite complexes in the Arabian Shield, *Precambrian Res.* **19:** 31-50.

Murthy, V.R. and **Griffin, W.L.** (1970) K/Rb fractionation by plagioclase feldspars, *Chem. Geol.* **6:** 265-271.

Nasseef, A.O. and **Gass, I.G.** (1980) Arabian Shield granite traverse, *Inst. Appl. Geol. (Jeddah), Bull.* 3(4): 77-82.

O'Connor, J.T. (1965) A classification of quartz rich igneous rocks based on feldspar ratios, *U.S. Geol. Surv., Prof. Paper* **525B:** B79-B84.

Pankhurst, R.J. and **O'Nions, R.K.** (1973) Determination of Rb/Sr and $^{87}Sr/^{86}Sr$ ratios of some standard rocks and evaluation of X-ray flourescence spectrometry in Rb-Sr geochemistry, *Chem. Geol.* **12:** 127-136.

Priem, H.N.A., Boelrijk, N.A.I.M., Hebeda, E.H., Schermerhorn, L.J.G., Verdurmen, E.A.Th. and **Verschure, R.H.** (1978) Sr-isotope homogenization through whole-rock systems under low greenschist facies metamorphism in Carboniferrous pyroclastics at Aljustrel (Southern-Portugal), *Chem. Geol.* **21:** 307-314.

Radain, A.A., Ali S., Nasseef, A.O. and **Abdel-Monem, A.A.,** (1987) Rb-Sr geochronology and geochemistry of plutonic rocks from the Wadi Shuqub quadrangle, West-Central Arabian Shield. *J. Afr. Earth. Sci.* **6:** 553-568

Radain, A.A. and **Nasseef, A.O.** (1982) Geochronology and geochemistry of Wadi Shuqub granitic rocks, west-central Arabian Shield, *Precambrian Res.* **16:** A 35 (Abstract).

Ramsay, C.R., Basahel, A.N. and **Jackson, N.J.** (1981) Petrography, geochemistry and origin of the volcano-sedimentary succession between Jabal Ibrahim and Al-Aqiq, Saudi Arabia. *Fac. Earth Sci., King Abdulaziz Univ., Bull.* **4:** 1-24.

Riofinex (1977) A preliminary review of mineral opportunities in Saudi Arabia. *Saudi Arabian Dir. Gen. Miner. Resour. Rept.* **RF-1977-1,** 186 p.

Roddick, J.C. and **Compston, W.** (1977) Strontium isotopic equilibration: a solution to a paradox. *Earth Planet. Sci. Lett.* **34:** 238-246.

Roobol, M.J., Ramsay, C.R., Jackson, N.J. and **Darbyshire, D.P.F.** (1983) Late Proterozoic lavas of the central Arabian Shield-evolution of an ancient volcanic arc system, *J. Geol. Soc. Lond.* **140:** 185-202.

Schmidt, D.L., Hadley, D.G., Greenwood, W.R., Gonzalez, L., Coleman, R.G. and **Brown, G.F.** (1973) Stratigraphy and tectonism of the southern part of the Precambrian Shield of Saudi Arabia, *Saudi Arabian Dir. Gen. Miner. Resour., Bull.* **8,** 13 p.

Shaw, D.M. (1968) A review of K/Rb fractionation trends by covariance analysis. *Geochim. Cosmochim. Acta* **32:** 573-602.

Sighinolfi, G.P. (1971) Investigation into deep crustal levels: fractionating effects and geochemical trends related to high-grade metamorphism, *Geochim. Cosmochim. Act.* **34:** 1005-1021.

Smalley, P.C., Field, D. and **Raheim, A.** (1983) Resetting of Rb-Sr whole-rock isochrons during sveconorwegian low-grade events in the Gjerstad augen gneiss, Telemark, southern Norway, *Isotope Geoscience* **1:** 269-282.

Steiger, R.H. and **Jager, E.** (1977) Subcommission on geochronology: Convention on the use of decay constants in geo- and cosmo-chronology, *Earth Planet. Sci. Lett.* **36:** 359-362.

Stoeser, D.B. and **Camp, V.E.** (1984) Pan-African microplate accretion of the Arabian Shield, *Saudi Arabian Deputy Ministry for Mineral Resources., Tech. Record.* **USGS-TR-04-17,** 26 p.

Tarney, J. and **Windley, B.F.** (1977) Chemistry, thermal gradients and evolution of the lower continental crust, *J. Geol. Soc. Lond.* **134:** 153-172.

Taylor, S.R. (1966) The application of trace element data to problems in petrology, *Phys. and Chem. Earth* **6:** 133-213.

Thornton, C.P. and **Tuttle, O.F.** (1960) Chemistry of igneous rocks. 1, Differentiation index, *Am. J. Sci.* **258:** 664-684.

Turner, F.J. (1980) Metamorphic Petrology, 2nd edition, McGraw-Hill, New York, 512 p.

Turner, F.J. and **Verhoogen, J.** (1960) *Igneous and Metamorphic Petrology*, McGraw-Hill, New York, 694 p.

Tuttle, O.F. and **Bowen, N.L.** (1958) Origin of granites in the light of experimental studies in the system $NaAlSi_3O_8$-$KAlSi_3O_8$-SiO_2, *Geol. Soc. Am. Mem.* **74,** 153 p.

Wickman, F.E., Aberg, G. and **Beatriz, L.** (1983) Rb-Sr dating of alteration events in granitoids, *Contrib. Mineral. Petrol.* **83:** 358-362.

York, D. (1969) Least-squares fitting of a straight line with correlated errors, *Earth Planet. Sci. Lett.* **5:** 320-324.

التأريخ الجيولوجي والتطور الجيوكيميائي لمعقَّد وادي تُرَبة الفِلْسي السحيقي الحلقي ، وسط الدِّرع العربي

عبد العزيز رادين ، سيد علي وعبد الله عبد المنعم
كلية علوم الأرض – جامعة الملك عبد العزيز
جدة – المملكة العربية السعودية

يناقش هذا البحث أيزوكرونات الروبيديوم/استرنشيوم لكامل الصخر ومعطيات تحليل الأكاسيد الرئيسة في الصخور الفِلْسية السحيقية لمعقَّد وادي تربة الحلقي . وتبين الصخور الفلسية لمركب وادي تربة تاريخا تطوريا معقدا حيث تتكون من صحبة جرانوديوريت نيسي (GGGS) وصحبة جرانوديوريت كُتلي (MGGS) ، بالإضافة إلى الجرانيت القاطع الحلقي . وتعرضت الصحبة الأولى (GGGS) بالإضافة إلى الصخور البركانية والرسوبية المتحولة والمتطبقة الضاربة إلى الشمال والمقسمة في مجموعتي بيش وباحة ، والتي تعرضت إلى تشوه عديد المراحل وتحول إلى الرتب العليا والمنخفضة من سحنات الشست الأخضر والأمفيبوليت ، على التوالي . ويمثل جرانيت القاطع الحلقي المرحلة الأخيرة في التطور الصهاري للمعقد الحلقي .

حددت بيانات الروبيديوم/استرنشيوم لكامل الصخر في ٦ عينات من الصحبة (GGGS) عمرا ظاهريا هو ٥٣٥ ± ١١ مليون سنة (٢ σ) مع نسبة استرنشيوم ٨٧/استرنشيوم ٨٦ إبتدائية ٧٠٣٧ر٠٠ ± ٠٠٠١٦ر٠ (٢ σ) وقيمة (MSWD) ٦ر٦ . أما العمر المحدد على ٥ عينات من الصحبة (MGGS) فكان ٤١٦ ± ٩ مليون سنة (٢ σ) مع نسبة ابتدائية ٧٠٤ر٠ ± ٠٠٠٢ر٠ (٢ σ) و MSWD ٩ر٠١ وأعطى الجرانيت القاطع الحلقي عمرا أيزوكرنيا مع أربع نقاط وصل إلى ١١٧ ± ٤ر٠ مليون سنة مع نسبة ابتدائية ٧٠٨٩ر. ± ٠٠٠٠٢ر٠ (٢ σ) وقيمة MSWD ٠١ر٠ .

وتدل معطيات أكاسيد العناصر الرئيسة والروبيديوم/استرنشيوم على أن الصخور الفلسية السحيقة الموجودة في المركب الحلقي شديدة التفارق اشتقت بالتبلور التجزيئي لصهارة نشأت من القشرة السفلى أو الوشاح العلوي ، كما دلت المعطيات الكيميائية على أن جرانيت القاطع الحلقي متفاصل من صهارة تمثل التركيب الأدنى في النظام الثلاثي SiO_2 KAl SiO_4- NaAl SiO_4 وتحت ضغط ماء بلغ كيلو بار واحد .